Thermochemical Parameters and Growth Mechanism of the Boron− Doped Silicon Clusters, SinBq With n = 1 − 10 and q = −1, 0, +1

ARTICLE *in* THE JOURNAL OF PHYSICAL CHEMISTRY C · AUGUST 2012

Impact Factor: 4.77 · DOI: 10.1021/jp306037q

3 AUTHORS:

Tam Minh Nguyen
University of Leuven
20 PUBLICATIONS **136** CITATIONS
SEE PROFILE

Truong Tai
University of Leuven
65 PUBLICATIONS **506** CITATIONS
SEE PROFILE

Minh Tho Nguyen
University of Leuven
748 PUBLICATIONS **10,835** CITATIONS
SEE PROFILE

THE JOURNAL OF PHYSICAL CHEMISTRY C

Article

pubs.acs.org/JPCC

Thermochemical Parameters and Growth Mechanism of the Boron-Doped Silicon Clusters, Si_nB^q with $n = 1-10$ and $q = -1, 0, +1$

Nguyen Minh Tam,[†,‡] Truong Ba Tai,[†] and Minh Tho Nguyen*[,†]

[†]Department of Chemistry, University of Leuven, B-3001 Leuven, Belgium

[‡]Institute for Computational Science and Technology at HoChiMinh City (ICST), QuangTrung Software Park, Ho Chi Minh City, Vietnam

Supporting Information

ABSTRACT: A systematic investigation of the boron-doped silicon clusters Si_nB with n ranging from 1 to 10 in the neutral, anionic, and cationic states is performed using quantum chemical calculations. Lowest-energy minima of the clusters considered are identified on the basis of the B3LYP, G4, and CCSD(T) energies. Total atomization energies and thermochemical properties such as ionization energy, electron affinity, and dissociation energies are obtained using the high accuracy G4 (B3LYP-MP4-CCSD(T)) and CCSD(T)/CBS (complete basis set up to $n = 4$) methods. Theoretical heats of formation are close to each other and used to assess the available experimental values. The growth mechanism for boron-doped silicon clusters Si_nB with $n = 1-10$ emerges as follows: (i) each Si_nB cluster is formed by adding one excess Si-atom into the smaller sized $Si_{n-1}B$, rather than by adding B into Si_n, (ii) a competition between the exposed (exohedral) and enclosed (endohedral) structures occurs at the size Si_8B where both structures become close in energy, and (iii) the larger size clusters Si_9B and $Si_{10}B$ exhibit endohedral structures where the B-impurity is located at the center of the corresponding Si_n cages. The species Si_9B^-, Si_9B, and $Si_{10}B^+$ are identified as enhanced stability systems with larger average binding energies and embedded energies. The higher stability of the closed shells Si_9B^- and $Si_{10}B^+$ can be rationalized in terms of the jellium electron shell model and spherical aromaticity.

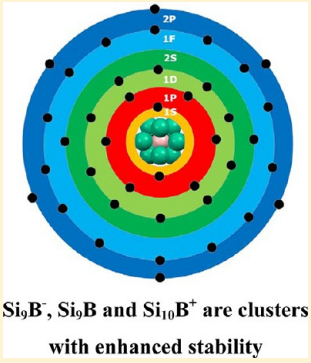

Si_9B^-, Si_9B and $Si_{10}B^+$ are clusters with enhanced stability

INTRODUCTION

Numerous experimental and theoretical studies recently reported in the literature leave no doubt for a considerable interest in silicon-based clusters. Unlike carbon whose small clusters tend to form linear or planar cyclic structures with sp^2-hybridized atom, silicon favors sp^3-like bonding and forms three-dimensional structures. Small pure silicon clusters Si_n^q in various charged states ($q = -1, 0, 1$) were found to exhibit structural characteristics similar to those of the corresponding well-known boron hydrides.[1]

Since the first experimental observation showing the existence of the endohedral transition metal-doped silicon clusters,[2] a large number of investigations on doped silicon clusters have been reported.[3−35] Recently, some of us carried out a number of combined experimental and theoretical studies on metal-doped silicon clusters Si_nM with M = Li, Cu, V.[35,36] Our findings pointed out among other things that while Li and Cu atoms prefer to be absorbed on the surface of silicon hosts, the V-doped silicon clusters are built up by substituting one Si-atom of the Si_n frameworks by the dopant V-atom. Similar observations were also found for other small impure silicon clusters Si_nM in that the impurities M either adsorb on the surface or substitute one of the Si-atoms of the Si_n-parents. Perhaps more interestingly, Ngan and Nguyen[37] recently found that the species $M@Si_8^q$ containing 34 valence electrons possess the perfect octahedral structures in which the impurities M (Be, B, C, N, etc., with appropriate positive charge) are located at the center of the Si_8 cube. These species apparently exhibit the intriguing features of a cubic aromaticity with 8 valence electrons that satisfy the electronic shell model. However, because of the lack of results on the other sizes, the thermodynamical stability of these systems has not been examined. We should note that the closed shell impure clusters with compact and high symmetry structures are of current interest because they can be used as building blocks for self-assembling nanomaterials. Such endohedral structures were recently observed for the group IVA doped clusters such as $M@Ge_n$, $M@Sn_n$, and $M@Pb_n$ with $n = 10$, 12, and 14.[38−40] However, endohedral $M@Si_n$ clusters are rather scarce, in part due to the fact that the size of the similar Si_n cages remains small to enclose the M impurities. As a consequence, the existence of the $M@Si_8$ species prompts us to find more evidence for the stable $M@Si_n$ clusters containing the light dopants such as Be, B, C, etc.

Boron−silicon compounds have also attracted much attention in part due to their important applications in microelectronic fields. Boron is the most important element widely used to date as a p-type dopant in crystalline silicon. Earlier studies showed that when the concentration of boron is increased, formation of either a silicon boride phase or Si−B

Received: June 19, 2012
Revised: August 11, 2012

   dx.doi.org/10.1021/jp306037q | J. Phys. Chem. C XXXX, XXX, XXX−XXX

clusters occurs in crystalline Si.[41,42] These solid materials are also known for their mechanical hardness. However, despite the demonstrated importance of the boron−silicon compounds, an understanding of their electronic and thermodynamic properties is still very limited. According to our best knowledge, only a few studies on small Si_nB clusters were reported. The heats of formation of gas-phase small Si_nB clusters with n = 1−3 were measured by Viswanathan et al.[43] Davy et al.[44] performed a theoretical study on the structure, energy, and vibration spectra of the small mixed species B_2Si, B_2Si_2, and BSi_2 using molecular orbital (MO) calculations. More recently, a combined experimental and theoretical study on small anionic Si_nB^- and Si_nAl^- clusters with n = 1−6 was carried out by Sun et al.[45] using time-of-flight mass spectrometry and density functional theory (DFT) calculations. It is surprising that the larger clusters Si_nB have not been examined yet. In this context, an investigation on Si_nB clusters in various charge states appears necessary to gain more insights into the structural features and fundamental properties of these intriguing systems.

Motivated by the above reasons, we set out to carry out a systematic investigation on a series of small boron-doped silicon clusters Si_nB with n = 1−10 in the cationic, neutral, and anionic states using both DFT and MO methods. Thermochemical properties of clusters considered are calculated by using the composite G4 and CCSD(T)/CBS (complete basis set) approaches that were effectively used in our recent studies on silicon-doped boron clusters B_nSi.[46] Our theoretical predictions on the growth pattern point out that the closed shell systems $Si_{10}B^+$ and Si_9B^- are characterized by an enhanced stability with spherical aromaticity features. Their high thermodynamic stabilities can consistently be rationalized in terms of the electron shell model.

COMPUTATIONAL METHODS

All electronic structure calculations were carried out using the Gaussian 09[47] and Molpro 2008[48] program packages. Previous investigations on mixed Si_nM clusters indicated that the dopant M either adsorbs on the surface or substitutes one of the Si-atoms of a Si_{n+1} cluster. On this basis, the trial structures of Si_nB are generated by two ways: (i) addition of a B-atom at different positions around the well-known geometric structures of the bare anionic, cationic, and neutral silicon $Si_n^{-/0/+}$ clusters, and (ii) substitution by a B-atom at a Si position of the Si_{n+1} parents. Their geometries then are fully optimized. In addition, other alternative structures of the doped silicon clusters previously reported are also used as initial structures for geometry optimizations at the B3LYP/6-31G(d) level.[49,50] Thanks to the fact that the structures of small pure and impure silicon clusters were well established in previous studies, our simple but careful and extensive search method allows us to determine the most stable equilibrium structures of the Si_nB clusters considered. Geometries and vibrational frequencies of the converged equilibrium structures Si_nB and their anions and cations are subsequently reoptimized using again the hybrid B3LYP functional but in conjunction with the larger 6-311+G(d) atomic basis set.[51−53]

Standard enthalpies of formation of the global minima are evaluated from the corresponding total atomization energies (TAE).[54] For this parameter, two sets of calculations are performed, including the coupled-cluster theory with complete basis set approach CCSD(T)/CBS, as previously used for the series of small boron clusters,[55] and the composite G4 approach[56] in which the geometry optimizations and calculations of harmonic vibrational frequencies are carried out at the B3LYP/6-31G(2df,p) level, followed by combined fourth-order perturbation theory MP4(SDTQ) and coupled-cluster theory CCSD(T) single point energy calculations using the additivity approximation for contributions of different basis sets.

In the CCSD(T)/CBS approach, geometrical parameters are fully optimized using the coupled-cluster CCSD(T) theory[57] along with the correlation consistent aug-cc-pVTZ basis set.[58] Single-point electronic energies are subsequently calculated using the restricted/unrestricted coupled-cluster (R/UCCSD-(T)) formalism[59,60] with the aug-cc-pVnZ (n = Q and 5) basis sets[58] and then extrapolated to the complete basis set limit (CBS). For simplicity, the basis sets are labeled as aVnZ. The CCSD(T) energies are extrapolated to the CBS limit energies using expression 1:[61]

$$E(x) = E_{CBS} + B/x^3 \quad (1)$$

where x = 4 and 5 for the aVnZ basis with n = Q and 5, respectively. Total CCSD(T) electronic energies as a function of basis set are given in Table S1 of the Supporting Information. Additional smaller corrections are also included in the TAE evaluations. Core−valence corrections (ΔE_{CV}) are obtained at the CCSD(T)/aug-cc-pwCVTZ level of theory.[62] Douglas−Kroll−Hess (DKH) scalar relativistic corrections ($\Delta E_{DKH\text{-}SR}$), which account for changes due to relativistic contributions to total energies of the molecule and constituent atoms, are calculated using the spin-free, one-electron DKH Hamiltonian.[63−65] $\Delta E_{DKH\text{-}SR}$ is defined as the difference in the atomization energy between the results obtained from basis sets recontracted for DKH calculations and the atomization energy obtained with the normal valence basis set of the same quality. The DKH calculations are obtained as the differences of the results from the CCSD(T)/cc-pVTZ and the CCSD(T)/cc-pVTZ-DK levels of theory. Finally, a spin−orbit (SO) correction of 0.03 kcal/mol for the B atom and 0.43 kcal/mol for the Si atom are obtained from the excitation energies of Moore.[66] The total atomization energy ($\sum D_0$ or TAE) of a compound is given by expression 2:

$$\sum D_0 = \Delta E_{elec}(CBS) + \Delta E_{CV} + \Delta E_{DKH\text{-}SR} + \Delta E_{SO} - \Delta E_{ZPE} \quad (2)$$

By combining our computed $\sum D_0$ values determined from either the CBS or the G4 calculations, with the known experimental heats of formation at 0 K for the elements B and Si, we can derive ΔH_f° values at 0 K for the molecules in the gas phase. In this work, we use the values at 0 K $\Delta H_f^\circ(B)$ = 135.1 ± 0.2 kcal/mol, and $\Delta H_f^\circ(Si)$ = 107.2 ± 0.2 kcal/mol.[67] We subsequently obtain the heats of formation at 298 K by following the classical thermochemical procedure.[68] The calculated heats of formation at 0 K are used to evaluate the adiabatic ionization energy (IE), electron affinity (EA), and other energetic quantities. Because of our limited computational resources, CBS calculations are performed only for the smallest molecules Si_nB with n = 1−4. The G4 approach is therefore used for the entire series considered.

RESULTS AND DISCUSSION

The shapes of the equilibrium structures of the neutral Si_nB, cationic Si_nB^+, and anionic Si_nB^- systems, their relative energies obtained using both B3LYP and G4 methods, and symmetry point groups are shown in Figures 1, 2, 3, and 4. The different

dx.doi.org/10.1021/jp306037q | J. Phys. Chem. C XXXX, XXX, XXX−XXX

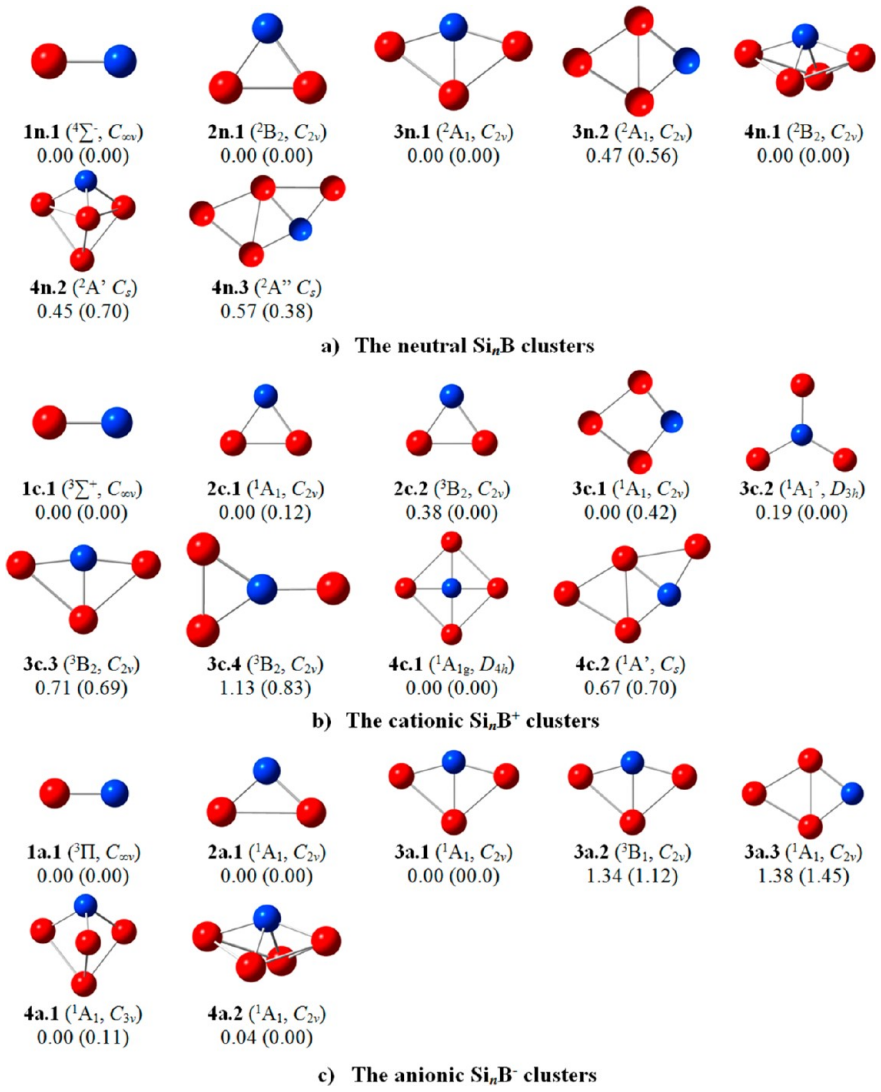

Figure 1. Shapes, electronic states, and relative energies (ΔE, eV) of the lower-lying isomers Si_nB with n = 1−4 at the (a) neutral, (b) cationic, and (c) anionic states. ΔE values are obtained at the G4 approach. Values given in brackets are from B3LYP/6-311+G(d)+ZPE computations.

components obtained in the CBS protocol for evaluating their total atomization energies ($\sum D_0$) are given in Table 1, whereas the total CBS energies for small sized clusters $Si_nB^{+/0/-}$ with n = 1−4 and total G4 energies for all lowest-energy structures $Si_nB^{+/0/-}$ are summarized in Tables S1 and S2 of the Supporting Information. The heats of formation of the clusters derived using the $\sum D_0$ obtained from both CBS and G4 methods are given in Table 2. The computed adiabatic ionization energies (IEs) and adiabatic electron affinities (EAs) of B_nSi clusters are listed in Table 3. The average binding energies (E_b) and embedded energy (EE) are tabulated in Table 4.

Thermochemical Properties of Clusters. At first glance, there is a reasonable agreement between both sets of CBS and G4 results (Table 1). The heats of formation at 0 K (ΔH^0_f) obtained by the CBS method are larger than those obtained applying the composite G4 approach (Table 2). The difference varies in the range of 0.9−5.8 kcal/mol. The adiabatic IE is obtained from the energy difference between the neutral Si_nB and its corresponding Si_nB^+ cation, whereas the adiabatic EA corresponds to the energy difference between the neutral Si_nB and its Si_nB^- anion. The values given in Table 3 also reveal a better agreement between both theoretical approaches. The maximum difference between both sets of values is 0.11 eV for EAs and 0.12 eV for IEs. These differences of energetic values between both G4 and CBS methods can be understood from the ways of computing single point electronic energies, as well as the geometries of clusters used. While geometries are obtained, as mentioned above, at the CCSD(T)/aug-cc-pVTZ level for the CBS method, the G4 approach actually uses geometries obtained at the B3LYP/6-31G(2df,p) level.

More importantly, both methods show a good agreement with available experimental data. The heats of formation of diatomic SiB obtained from the G4 and CBS methods amount to 167.1 and 167.9 kcal/mol, respectively, that agree well with the experimental value of 165.87 ± 3.35 kcal/mol,[43] which was determined by using Knudsen cell mass spectrometry and thermal functions. A similar observation is found for the triatomic Si_2B whose experimental heat of formation of 163.72 ± 4.78 kcal/mol[43] is somewhat larger than the G4 value of 162.9 kcal/mol but slightly smaller than the CBS value of 164.3 kcal/mol. The computed heats of formation of 174.8 (G4) and 176.4 (CBS) kcal/mol for Si_3B are significantly larger than its available experimental value of 167.06 ± 7.41,[43] but they are

dx.doi.org/10.1021/jp306037q | J. Phys. Chem. C XXXX, XXX, XXX−XXX

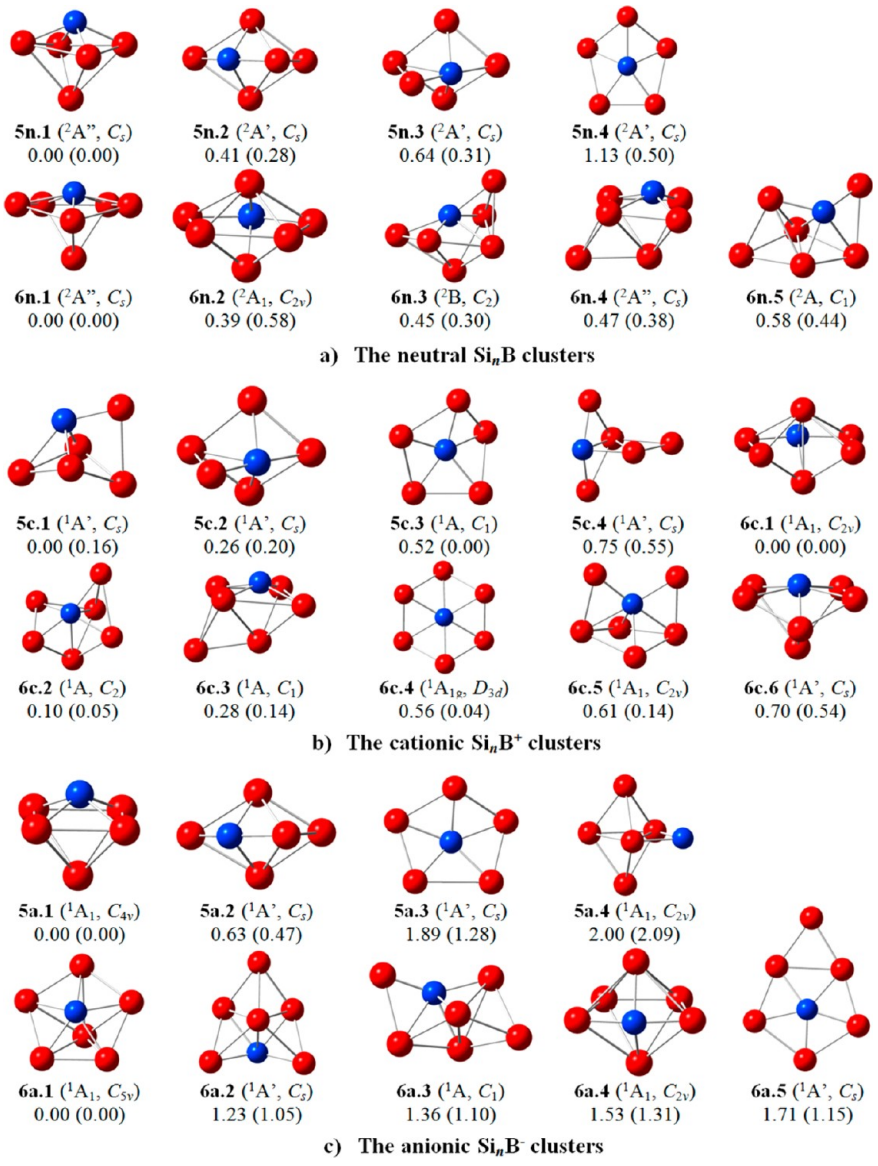

Figure 2. Shapes, electronic states, and relative energies (ΔE, eV) of the lower-lying isomers Si_nB with n = 5 and 6 at the (a) neutral, (b) cationic, and (c) anionic states. ΔE values are obtained at the G4 approach. Values given in brackets are from B3LYP/6-311+G(d)+ZPE computations.

also situated within the error bar of ±7.41 kcal/mol. This agreement lends us confidence in thermochemical parameters predicted for the remaining clusters. The G4 values thus provide us with a consistent set of heats of formation for the whole series of Si_nB clusters in three charge states, and they can be used for the systems whose experimental data are not determined yet.

Lower-Lying Isomers of Si_nB Clusters and Their Growth Mechanism. As mentioned above, a large number of isomeric equilibrium structures are located for each of the clusters considered. In this Article, we only present some lower-lying isomers whose relative energies are close to the ground states (within 1.0 eV). As for a convention, each structure described hereafter is defined by the label ***n*X.*Y*** in which ***n*** is the size of Si_n, ***X*** = **n, c, a** stands for a neutral, cation, or anion, respectively, and **Y** = **1, 2...** indicates the energy ordering of the isomer considered. We first describe briefly the situation in each size, followed by an analysis of their growth pattern.

n = **1**: SiB, SiB^+, and SiB^-. In good agreement with earlier reports,[69] our calculations show that the diatomic SiB is characterized by the high spin **1n.1** with the $^4\sum^-$: $[1\sigma^2 2\sigma^2 1\pi^2 3\sigma^1]$ valence electronic configuration. Following attachment of one excess electron into π bonding orbital, the high spin state **1a.1** $^3\Pi$: $[1\sigma^2 2\sigma^2 1\pi^2 2\pi^1 3\sigma^1]$ becomes the ground state of SiB^-. A more detailed description for these species can be found in our recent report. The cationic diatomic SiB^+ is found to be the triplet **1c.1** with valence electronic configuration of $^3\sum^+$: $[1\sigma^2 2\sigma^2 1\pi^2 3\sigma^0]$.

n = **2**: Si_2B, Si_2B^+, and Si_2B^-. Si_2B has a triangular ground state **2n.1** (C_{2v}, $^2B_2$) in which the B atom connects with two Si-atoms. Following either attachment or detachment of one electron to form the charge species, the shape of the resulting ions remains almost unchanged. Both the cation Si_2B^+ and the anion Si_2B^- exhibit the C_{2v} ($^1A_1$) structures **2c.1** and **2a.2** with closed shell electronic configurations (Figure 1).

n = **3**: Si_3B, Si_3B^+, and Si_3B^-. Si_3B has a C_{2v} ($^2A_1$) ground state **3n.1** in which the third Si atom is connected with a Si−B edge of **2n.1** rather than with a Si−Si edge. The next isomer is another C_{2v} ($^2A_1$) structure **3n.2** with a relative energy of 0.47 eV, which is formed from the latter motif where the third Si-

dx.doi.org/10.1021/jp306037q | J. Phys. Chem. C XXXX, XXX, XXX−XXX

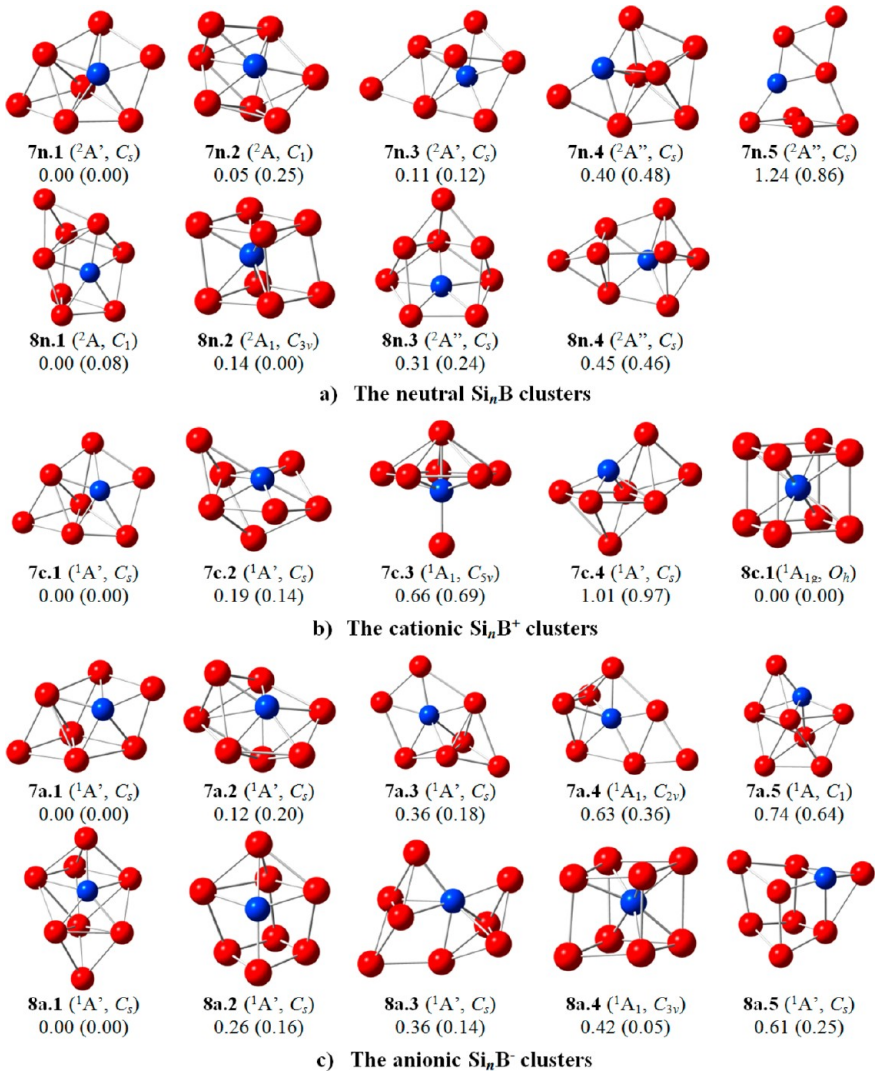

Figure 3. Shapes, electronic states, and relative energies (ΔE, eV) of the lower-lying isomers Si_nB with n = 7−8 at the (a) neutral, (b) cationic, and (c) anionic states. ΔE values are from G4 computations, whereas values given in brackets are obtained at the B3LYP/6-311+G(d)+ZPE level.

atom is connected with the Si−Si edge of **2n.1**. There is a negligible difference in geometries of the anion Si_3B^- and cation Si_3B^+ as compared to their neutral counterpart. The structure **3a.1** (C_{2v}, $^1A_1$) is found to be the global minimum of Si_3B^-. The remaining isomers are at least 1.34 eV less stable than **3a.1** (Figure 1).

At the B3LYP/6-311+G(d) level, a high symmetry structure **3c.2** (D_{3h}, $^1A_1'$) in which the B-impurity is located at the center of a Si_3 triangle is calculated to be the lowest-energy isomer for the cation Si_3B^+. The next isomer is a C_{2v} $^1A_1$ structure **3c.1** that has the shape of the corresponding neutral **3n.1**. However, G4 calculations point out a reversed energy ordering that **3c.1** is now the most stable isomer with energy gap of 0.19 eV below **3c.2**. Two triplet states **3c.3** and **3c.4** are also located as local minima with 0.71 and 1.13 eV higher in energy as compared to **3c.1** (Figure 1).

n = **4**: Si_4B, Si_4B^+, and Si_4B^-. Interestingly, the Si_4B^+ cation exhibits a perfect squared form **4c.1** (D_{4h}, $^1A_1'$) in which B-atom is located at the center of a Si_4 square (Figure 1). This isomer can be formed by directly binding one Si atom to the B atom of **3n.1**. The shape of molecular orbitals of **4c.1** reveals that its LUMO and LUMO+1 are degenerate. Consequently, following attachment of one excess electron, the geometry of the corresponding neutral is distorted under a Jahn−Teller effect. The structure **4n.1** (C_{2v}, $^2B_2$) in which the B atom is distorted out of the structural plane of **4c.1** is found to be the global minimum for Si_4B. On the basis of G4 calculations, the three-dimensional (3D) form **4n.2** is the next isomer that is 0.45 eV less stable than the global minimum. A planar form **4n.3** that is formed by connecting the fourth Si atom with the Si−Si edge of **3n.1** is also located with a relative energy of 0.57 eV.

In the anionic state, there is an interesting competition in energy between both isomers **4a.1** and **4a.2**. At the B3LYP/6-311+G(d) level, **4a.2** is the lowest-lying isomer, being 0.11 eV more stable than **4a.1**. However, our G4 results show a reversed energy ordering in that **4a.1** is now the most stable isomer, being only 0.04 eV lower in energy than **4a.2**. This gap is decreased to 0.026 eV from CCSD(T)/aug-cc-pVTZ calculated results. Thus, we can conclude that both structures likely exist as degenerate equilibrium ground states for the anion Si_4B^-.

n = **5**: Si_5B, Si_5B^+, and Si_5B^-. The most stable form of Si_5B is a 3D structure **5n.1** (C_s, $^2A''$) in which the new Si atom is located on the C4 axis and bound to four Si-atoms of **4n.1**. The second isomer is a C_s structure **5n.2** that is 0.41 eV higher in

dx.doi.org/10.1021/jp306037q | J. Phys. Chem. C XXXX, XXX, XXX−XXX

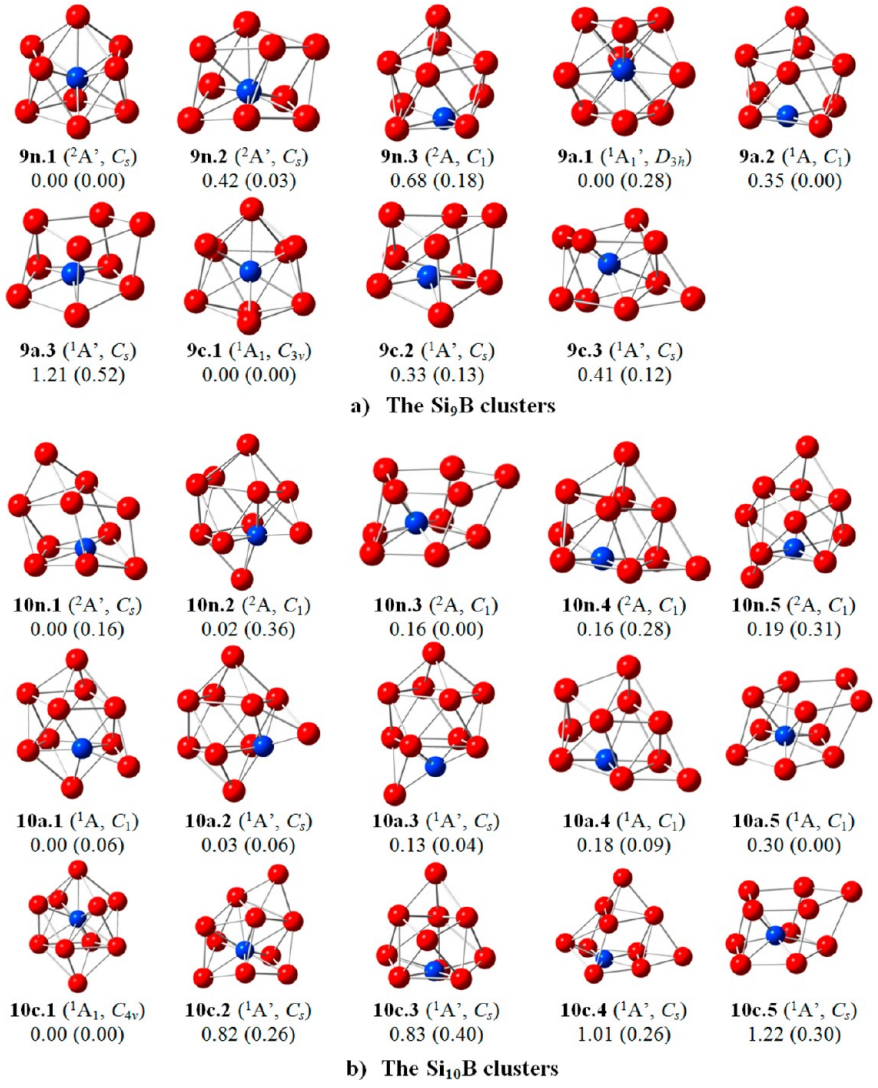

Figure 4. Shapes, electronic states, and relative energies (ΔE, eV) of the lower-lying isomers of (a) Si_9B and (b) $Si_{10}B$. ΔE values are obtained at the G4 approach. Values given in brackets are obtained at the B3LYP/6-311+G(d)+ZPE level.

Table 1. Total Atomization Energies ($\sum D_0$, TAE, kcal/mol) for Si_nB Clusters (n = 1−4) and Different Components of CCSD(T)/CBS Computations

structure	state	ΔCBS[a]	E_{ZPE}[b]	ΔE_{CV}[c]	ΔE_{SR}[d]	ΔE_{SO}[e]	$\sum D_0$ (TAE)
1a.1	$^3\Pi$	114.13	1.12	0.60	−0.26	−0.46	112.88
1n.1	$^4\sum^-$	75.37	1.05	0.63	−0.11	−0.46	74.37
1c.1	$^3\sum^+$	−132.83	1.00	0.31	0.04	−0.46	−133.94
2a.1	$^1A_1$	243.88	2.74	1.27	−0.55	−0.89	240.97
2n.1	$^2B_2$	187.55	2.52	1.41	−0.39	−0.89	185.17
2c.1	$^1A_1$	−10.37	2.22	0.90	0.24	−0.89	−12.34
3a.1	$^1A_1$	350.73	3.98	1.80	−0.80	−1.32	346.43
3n.1	$^2A_1$	284.17	3.78	1.88	−0.64	−1.32	280.31
3c.1	$^1A_1$	108.76	3.87	1.57	−0.32	−1.32	104.82
4a.1	$^1A_1$	449.37	5.34	2.44	−0.93	−1.75	443.79
4n.1	$^2B_2$	386.46	5.25	2.83	−0.75	−1.75	381.55
4c.1	$^1A_{1g}$	216.14	4.63	3.00	−0.25	−1.75	212.52

[a]Extrapolated by using eq 1 with the aVQZ and aV5Z basis sets. [b]Zero-point energies taken from the CCSD(T) harmonic frequencies. [c]Core−valence corrections obtained with the aug-cc-pwCVTZ basis set at the optimized CCSD(T) geometries. [d]Scalar relativistic corrections based on CCSD(T)-DK/cc-pVTZ-DK calculations and expressed relative to the CCSD(T) results without DK corrections. [e]Corrections due to the incorrect treatment of the atomic asymptotes as an average of spin multiplets. Values based on Moore's Tables, ref 66.

dx.doi.org/10.1021/jp306037q | J. Phys. Chem. C XXXX, XXX, XXX−XXX

Table 2. Heats of Formation at 0 K [ΔH_f (0 K)] and 298 K [ΔH_f (298 K)] (kcal/mol) of Si_nB in Neutral, Cationic, and Anionic States Obtained (G4 and CCSD(T)/CBS) in Their Lowest-Energy Forms

	ΔH_f (0 K)			ΔH_f (298 K)		
structure	G4	CBS	exptl.[a]	G4	CBS	exptl.[a]
1a.1 ($C_{\infty v}$ $^3\Pi$)	128.11	129.42		129.19	130.49	
1n.1 ($C_{\infty v}$ $^4\Sigma^-$)	167.06	167.93	165.87 ± 3.35	168.15	169.01	166.82 ± 3.35
1c.1 ($C_{\infty v}$ $^3\Delta$)	378.12	376.24		379.22	377.34	
2a.1 (C_{2v} $^1A_1$)	105.80	108.53		106.78	109.50	
2n.1 (C_{2v} $^2B_2$)	162.92	164.33	163.72 ± 4.78	163.87	165.28	164.43 ± 4.78
2c.1 (C_{2v} $^1A_1$)	360.25	361.84		361.26	362.84	
3a.1 (C_{2v} $^1A_1$)	107.10	110.27		108.13	111.29	
3n.1 (C_{2v} $^2A_1$)	174.80	176.39	167.06 ± 7.41	175.85	177.43	167.54 ± 7.41
3c.1 (C_{2v} $^1A_1$)	350.56	351.88		351.59	352.88	
4a.1 (C_{3v} $^1A_1$)	114.29	120.11		115.25	121.01	
4n.1 (C_{2v} $^2B_2$)	178.99	182.35		180.20	183.45	
4c.1 (D_{4h} $^1A_{1g}$)	348.46	351.38		350.20	352.58	
5a.1 (C_{4v} $^1A_1$)	96.49			97.69		
5n.1 (C_s $^2A''$)	174.11			175.38		
5c.1 (C_s $^1A'$)	350.56			351.77		
6a.1 (C_{5v} $^1A_1$)	105.22			106.40		
6n.1 (C_s $^2A''$)	188.32			189.91		
6c.1 (C_{2v} $^1A_1$)	353.20			354.56		
7a.1 (C_s $^1A'$)	138.94			140.49		
7n.1 (C_s $^1A'$)	206.48			208.03		
7c.1 (C_s $^1A'$)	358.62			360.16		
8a.1 (C_s $^1A'$)	147.61			149.35		
8n.1 (C_1 ^2A)	222.52			224.54		
8c.1 (O_h $^1A_{1g}$)	363.72			365.02		
9a.1 (D_{3h} $^1A_1'$)	126.07			128.22		
9n.1 (C_s $^2A'$)	210.21			212.57		
9c.1 (C_{3v} $^1A_1$)	369.09			371.26		
10a.1 (C_1 ^1A)	164.52			166.73		
10n.1 (C_s $^2A'$)	235.70			238.06		
10c.1 (C_{4v} $^1A_1$)	358.01			360.38		

[a]Experimental values taken from ref 43.

Table 3. Adiabatic Ionization Energies (IE) and Electronic Affinities (EA) of Si_nB, n = 1−10, Using G4 and CCSD(T)/CBS Calculations

	IE (eV)[a]		EA (eV)[b]	
n	G4	CBS	G4	CBS
1	9.15	9.03	1.69	1.67
2	8.56	8.56	2.48	2.42
3	7.62	7.61	2.94	2.87
4	7.35	7.33	2.81	2.70
5	7.65		3.37	
6	7.15		3.60	
7	6.60		2.93	
8	6.12		3.25	
9	6.89		3.65	
10	5.30		3.09	

[a]Obtained from difference between heats of formation of ***n*n.1** and ***n*c.1** with n = 1−10. [b]Obtained from difference between heats of formation of ***n*a.1** and ***n*n.1** with n = 1−10.

Table 4. Average Binding Energies (E_b, eV) and Embedded Energies (EE, eV) of Si_nB^-, Si_nB, and Si_nB^+ clusters (G4 Calculations)

	E_b			EE		
n	Si_nB^-	Si_nB	Si_nB^+	Si_nB^-	Si_nB	Si_nB^+
1	1.80	1.63	1.13	3.60	3.26	2.25
2	3.07	2.70	2.56	5.05	4.86	4.20
3	3.45	3.06	3.19	5.34	4.72	5.39
4	3.63	3.34	3.50	5.24	4.62	5.27
5	3.93	3.59	3.67	6.07	5.21	5.72
6	3.98	3.65	3.80	6.08	4.63	5.24
7	3.88	3.68	3.87	5.10	4.09	5.52
8	3.92	3.71	3.94	5.80	5.11	6.10
9	4.09	3.86	3.98	7.17	5.70	6.53
10	3.99	3.83	4.09	4.93	4.19	6.84

energy. Remaining structures are much less stable, being at least 0.64 eV higher in energy.

Following attachment of one excess electron, the anion Si_5B^- turns out to have a high symmetry C_{4v} ($^1A_1$) structure **5a.1** that is similar to its neutral counterpart. Other isomeric anions are found to be at least 0.63 eV higher in energy as compared to **5a.1**. Interestingly, **5c.3** is calculated as the lowest-energy isomer of the cation Si_5B^+ at the B3LYP/6-311+G(d) level. Again, G4 results give rise to a reversed energy ordering in that **5c.1** is now the most stable isomer and located at 0.52 eV below **5c.3**. Thus, we could establish that **5c.1** is the lowest-energy form of the cation Si_5B^+.

***n* = 6**: Si_6B, Si_6B^+, and Si_6B^-. The Si_6B ground state is a low symmetry C_s ($^2A''$) structure **6n.1** that is formed by either adding one Si atom into the plane containing the four-

dx.doi.org/10.1021/jp306037q | J. Phys. Chem. C XXXX, XXX, XXX−XXX

membered ring of **5n.1** or adsorbing one Si-atom on the C5 axis of **5n.4**. A C_{2v} structure **6n.2**, which is formed by substituting a Si atom of the pentagon Si_7 framework by a B, is found to be the second-lying isomer with a large relative energy of 0.39 eV. Two other isomers **6n.3** and **6n.4** that can be derived by adding one Si atom on a different triangular faces of **5n.1** are the next isomers with relative energies of ∼0.45 eV.

There is a structural competition for Si_6B^+ cations. Accordingly, two structures including the C_{2v} **6c.1**, which is a distorted form of **6n.2**, and the C_2 **6c.2**, which is actually the cationic state of **6n.3**, are almost degenerate within an energy gap of 0.1 eV. The next isomer is the C_1 **6c.3** that corresponds to a **6n.4** cation. Although the high symmetry **6c.4** (D_{3d}) has a tiny energy gap of 0.04 eV at the B3LYP/6-311+G(d) level, G4 results point out that it is much less stable with a relative energy of 0.56 eV. The corresponding cationic species of **6n.1** is found to be much less stable with an energy gap of 0.70 eV.

The anion Si_6B^- is a perfect bipyramid pentagonal **6a.1**. Although some other isomers **6a.2**−**6a.5** are also located, they are at least 1.23 eV higher in energy.

n = **7**: Si_7B, Si_7B^+, and Si_7B^-. G4 results emphasize two degenerate structures **7n.1** and **7n.2** for the neutral Si_7B. They are formed by adding one Si on different triangular faces of the neutral **6n.1** (Figure 2). The isomer **7n.3** is also found to be quite stable, being at 0.11 (G4) and 0.12 (B3LYP) eV.

Following either an attachment or a detachment of one electron, the shapes of the resulting charged species Si_7B^+ and Si_7B^- are slightly distorted with respect to their neutral form. The ions **7c.1** and **7a.1**, which are distorted forms of **7n.1**, are the structures of the cation Si_7B^+ and anion Si_7B^-, respectively. The following isomers **7c.2** and **7a.2** are basically the cationic and anionic forms of **7n.2**. Other isomers are much less stable relative to their global minima.

n = **8**: Si_8B, Si_8B^+, and Si_8B^-. There is again a strong competition in bonding motifs for the Si_8B clusters. Two structures including **8n.1**, which is formed by adding the new Si on a triangular Si_3 face of **7n.2**, and a packing form **8n.2** in which B is located at the center of the cubic Si_8 form are almost degenerate in energy. The energy difference between them is only 0.08 eV (B3LYP/6-311+G(d)), and this gap is slightly increased to 0.14 eV in favor of **8n.1** by G4 calculations.

For anionic clusters, B3LYP calculations result in two degenerate structures **8a.1** and **8a.4** with an energy gap of only 0.05 eV. However, G4 results show that **8a.1** is the most stable isomer as this gap is increased up to 0.42 eV. The structure **8a.2**, which is formed by substituting one Si-atom of the bicapped pentagonal bipyramid Si_9 structure by one B, is rather stable being 0.26 eV higher in energy. The present computations thus confirm that in the cationic state, the perfect octahedral cube **8c.1** is the global minimum of Si_8B^+.[37] Other isomers are found to be much less stable than **8c.1**. We would refer to our previous paper[37] for a detailed analysis of the chemical bonding phenomenon and the special aromatic character of the cubic Si_8B^+.

n = **9**: Si_9B, Si_9B^+, and Si_9B^-. Our findings derived from G4 results indicate that the C_s $^2A'$ **9n.1** that is constructed by adding the entering Si on top of **8n.2** is the most stable isomer of Si_9B. This structure is similar to that of the Si_9Be reported by Kumar and Kawazoe in their series of studies on doped silicon clusters.[70] The C_s $^2A'$ **9n.2** in which B is situated inside of the Si_9 cage is almost degenerate at the B3LYP/6-311+G(d) level. Again, G4 calculations place the latter at 0.42 eV higher in energy relative to **9n.1**. The charged species **9a.1** and **9c.1** possess the same shape as their neutral, but with a higher symmetry.

n = **10**: $Si_{10}B$, $Si_{10}B^+$, and $Si_{10}B^-$. B3LYP/6-311+G(d) energies show that **10n.3** in which B is located inside a Si_{10} cage composed of two five-membered rings is the lowest-energy isomer. The next isomer is the C_s **10n.1** that is formed by attaching the additional Si on a triangular face of **9n.2** with 0.16 eV higher energy than **10n.3**, and the C_1 **10n.2** is located with a relative energy of 0.36 eV. As in the previous case, G4 results however indicate that **10n.1** is actually the most stable isomer of $Si_{10}B$ and **10n.2** is a quasi-degenerate, being only 0.02 eV higher in energy than **10n.1**. For its part, **10n.3** is now 0.16 eV higher in energy (G4). **10n.4** is formed by adding one Si on a triangular face of **9n.3** and also of low energy, being 0.16 eV above **10n.1** (G4).

The C_{4v} $^1A_1$ **10c.1** in which B is located at the center of a Si_{10} cage is the lowest-energy $Si_{10}B^+$. Interestingly, **10c.1** is again found to be similar to its isoelectronic species $Si_{10}Be$ reported earlier.[70a] Structures **10c.2** and **10c.5** that are the cationic forms of **10n.1** and **10n.2**, respectively, are now much less stable with a relative energy of 0.82 and 1.22 eV (G4).

For the anions $Si_{10}B^-$, five structures, **10a.1**−**10a.5**, are almost degenerate in energy within an energy separation of only 0.09 eV at the B3LYP/6-311+G(d) level. On the contrary, G4 computations suggest that the two structures **10a.1** and **10a.2** are the more stable among the isomers located.

Growth Pattern. On the basis of the structural features of the most stable forms identified above, the growth mechanism for the clusters Si_nB with n = 1−10 emerge as follows:

(i) Each boron-doped silicon cluster Si_nB is formed by adding the new Si atom into the smaller sized but doped cluster $Si_{n-1}B$. This motif appears to be more favored over the alternative in which the B atom attaches to the Si_n core.

(ii) A competition between the exposed (exohedral) and the enclosed (endohedral) structures appears to occur at the size n = 8 (Si_8B) where the exposed **8n.1** remains energetically preferred over the enclosed counterpart **8n.2** but the energy separation is getting small.

(iii) The larger size clusters Si_9B and $Si_{10}B$ definitely prefer an enclosed structure where the B-impurity is now doped inside the corresponding Si_n cage.

Relative Stability of Clusters. To probe the inherent stability of the clusters considered, the average binding energies (E_b) and embedded energies (EE) of clusters are examined. The average binding energies (E_b) can be defined as follows:

$$E_b(Si_nB) = [nE(Si) + E(B) - E(Si_nB)]/(n+1) \quad (3)$$

$$E_b(Si_nB^-) = [(n-1)E(Si) + E(Si^-) + E(B) - E(Si_nB^-)]/(n+1) \quad (4)$$

$$E_b(Si_nB^+) = [(n-1)E(Si) + E(Si^+) + E(B) - E(Si_nB^+)]/(n+1) \quad (5)$$

where $E(B)$, $E(Si)$, $E(Si^+)$, and $E(Si^-)$ are total energies of the B-atom, Si-atom, and the charged Si^+ and Si^-, respectively. $E(Si_nB)$, $E(Si_nB^+)$, and $E(Si_nB^-)$ are total energies of the clusters Si_nB at the neutral, cationic, and anionic states, respectively. All of these values are obtained from G4 calculations. The E_b values are summarized in Table 4, while their plots are depicted in Figure 5a. It can be seen that the E_b

dx.doi.org/10.1021/jp306037q | J. Phys. Chem. C XXXX, XXX, XXX−XXX

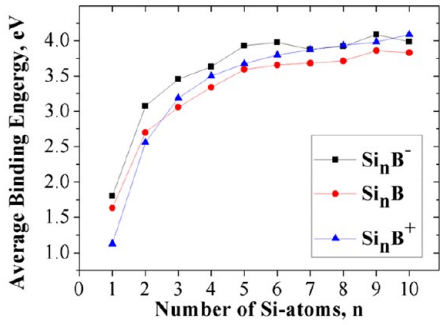

a) Plots of average binding energy (eV)

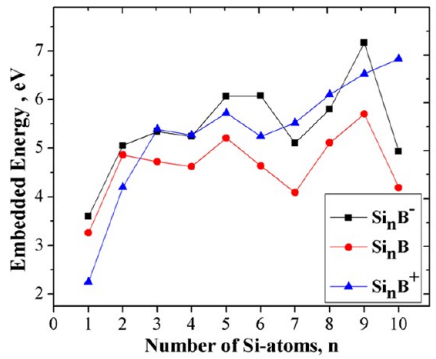

b) Plots of embedded energies (eV)

Figure 5. Average binding energy (E_b, eV) and embedded energies (EE, eV) of the $Si_nB^{+/0/-}$ clusters using the composite G4 method.

values tend to be increased with increasing cluster sizes. The $Si_{10}B^+$ cluster reveals the highest E_b value as compared to the smaller cationic Si_nB^+ species. At the neutral state, Si_9B presents the highest E_b value that indicates its high thermodynamical stability. Similarly, in the series of anions considered, it is Si_9B^- that gets a maximum peak in the E_b plot.

To confirm our above findings, the embedded energy (EE) of clusters is further examined. Embedding energy is the energy gain in incorporating B-impurity into the Si_n hosts and is defined as follows (eq 6):

$$EE(Si_nB^{-/0/+}) = E(Si_n^{-/0/+}) + E(B) - E(Si_nB^{-/0/+}) \quad (6)$$

where $E(Si_n^{-/0/+})$ are the total G4 energies of the anionic, neutral, and cationic Si_n clusters, respectively. These total G4 energies are calculated for the global minima of the pure clusters $Si_n^{0/\mp}$ reported in recent studies[12,71] and also given in Table S3 of the Supporting Information. Table 4 and Figure 5b show that Si_9B and Si_9B^- are indeed characterized by the highest EE values among the neutral Si_nB and anionic Si_nB^- clusters, respectively. These predictions agree well with the findings for the E_b values. Similarly, the cation $Si_{10}B^+$ again reveals the highest EE value as compared to other cationic species within the series. From these observations, we conclude that an enhanced thermodynamic stability is established for the species $Si_{10}B^+$, Si_9B, and Si_9B^-.

Dissociation Energies. To evaluate further the thermodynamic stability, the dissociation energies (D_e) for the various fragmentation channels of the clusters considered are determined. Results calculated from total G4 energies are shown in Table 5. Dissociation energies of the neutrals Si_nB for the Si-elimination channel (1) $Si_nB \rightarrow Si_{n-1}B + Si$ turn out to be smaller than those for the B-loss channel (2) $Si_nB \rightarrow Si_n + B$. This observation is consistent with the growth mechanism established above that a neutral Si_nB tends to be formed by attaching one extra Si into the smaller size $Si_{n-1}B$, rather than the alternative motif where the B-impurity is doped into the Si_n host. Similar observations are found for the charged species that the anionic Si_nB^- and cationic Si_nB^+ clusters tend to be fragmented to form one Si and a smaller anion $Si_{n-1}B^-$ along the fragmentation channel (3) and the cation $Si_{n-1}B^+$ along the channel (7), respectively.

More importantly, our calculations reveal that the clusters Si_9B, Si_9B^-, and $Si_{10}B^+$ exhibit the highest D_e values within the series of neutral, anionic, and cationic clusters, respectively. These results are internally consistent with the above discussion that these species constitute the enhanced stability systems among the clusters considered.

Enhanced Stability and Jellium Electron Shell Model (JSM). As for a rationalization of the relative stability of Si_nB clusters, we re-examine their MO pictures under the viewpoint of the jellium electron shell model (JSM),[72] which is applied successfully to interpret the stability motif of different types of atomic clusters in our recent reports.[37−40,73] According to this simple model in which the valence electrons are assumed to be freely itinerant in a simple mean-field potential formed by the nuclei of atoms, the valence electrons fill the spherical orbitals following the pattern of orbitals as $[1S^21P^61D^{10}2S^21F^{14}2P^61G^{18}2D^{10}...]$, etc. Within this model,

Table 5. Dissociation Energies (D_e, kcal/mol) for Various Fragmentation Channels of Si_nB in Neutral, Cationic, and Anionic States (G4 Calculations)[a]

	neutrals		anions				cations			
n	D_e (1)	D_e (2)	D_e (3)	D_e (4)	D_e (5)	D_e (6)	D_e (7)	D_e (8)	D_e (9)	D_e (10)
1	75.2	75.2	108.5	83.1	83.1	108.5	54.6	51.9	51.9	54.6
2	111.3	112.1	129.5	137.4	116.5	163.6	125.1	101.7	96.8	105.2
3	95.3	108.9	105.9	131.9	123.2	170.9	116.9	107.3	124.3	123.5
4	103.0	106.5	100.0	136.6	120.8	165.5	109.3	121.3	121.5	127.4
5	112.1	120.0	125.0	158.6	140.0	192.0	105.1	123.3	132.0	134.0
6	93.0	106.8	98.5	145.0	140.3	184.2	104.6	115.8	120.9	132.3
7	89.0	94.4	73.5	125.5	117.6	156.2	101.8	124.6	127.3	132.6
8	91.2	117.9	98.5	135.0	133.9	187.1	102.1	137.7	140.7	167.1
9	119.5	131.5	128.7	172.6	165.3	210.0	101.8	148.3	150.7	163.0
10	81.7	96.7	68.7	121.8	113.7	162.1	118.3	147.1	157.7	164.7

[a](1) $Si_nB \rightarrow Si_{n-1}B + Si$; (2) $Si_nB \rightarrow Si_n + B$; (3) $Si_nB^- \rightarrow Si_{n-1}B^- + Si$; (4) $Si_nB^- \rightarrow Si_{n-1}B + Si^-$; (5) $Si_nB^- \rightarrow Si_n^- + B$; (6) $Si_nB^- \rightarrow Si_n + B^-$; (7) $Si_nB^+ \rightarrow Si_{n-1}B^+ + Si$; (8) $Si_nB^+ \rightarrow Si_{n-1}B + Si^+$; (9) $Si_nB^+ \rightarrow Si_n^+ + B$; (10) $Si_nB^+ \rightarrow Si_n + B^+$.

dx.doi.org/10.1021/jp306037q | J. Phys. Chem. C XXXX, XXX, XXX−XXX

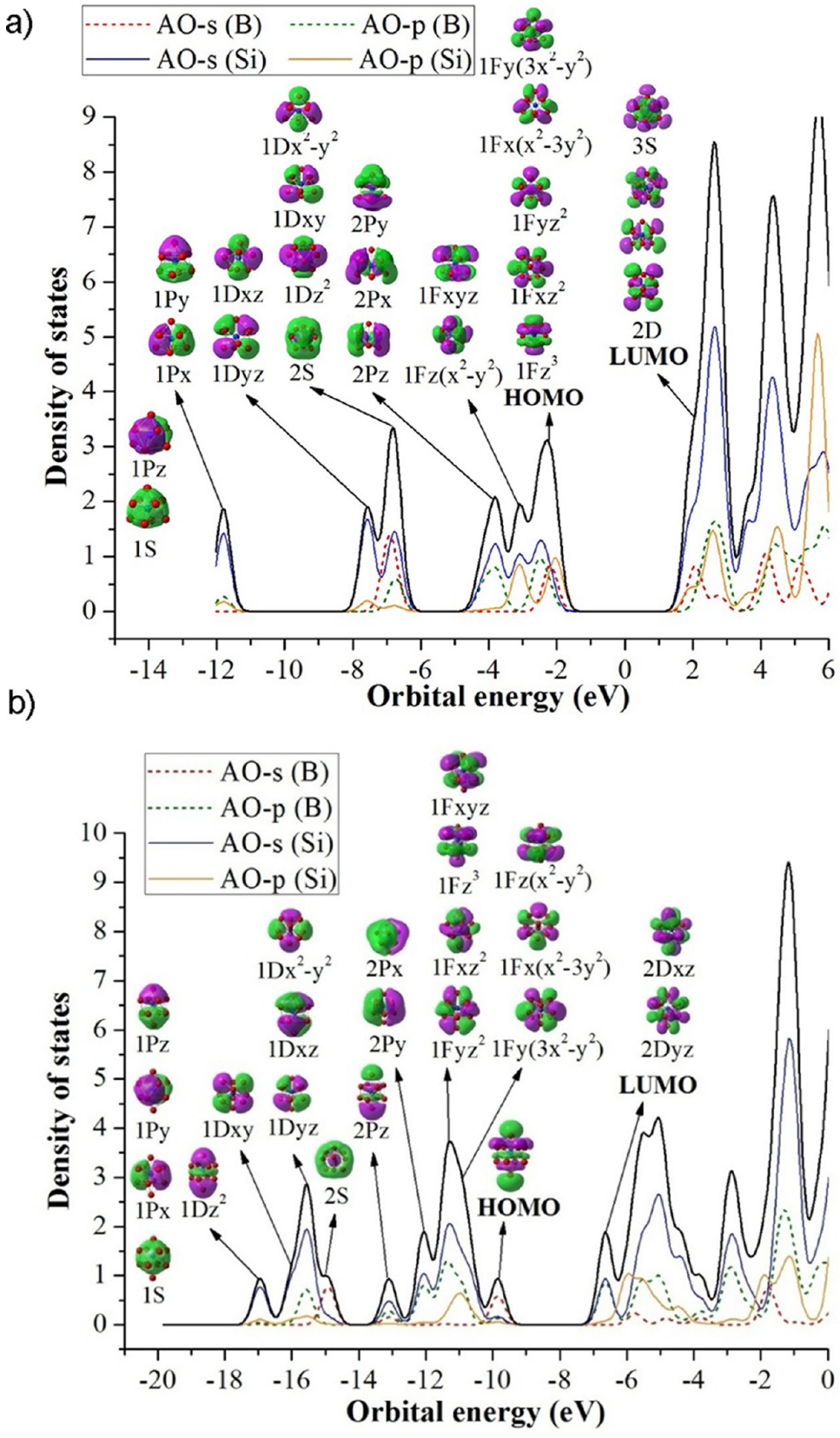

Figure 6. Total (DOS) and partial (pDOS) densities of state of (a) Si_9B^- and (b) $Si_{10}B^+$. The shapes of orbitals of clusters are obtained from B3LYP/6-311+G(d) calculations.

the number of electrons of 2, 8, 18, 20, 34, 40, 58, and 68, etc., emerge as the magic numbers that simply correspond to a complete filling of the successive shell electrons.

We should note that the observed number of closed shell electrons of a simple JSM is predicted on the basis of a spherical background. Thus, these magic numbers can eventually be

dx.doi.org/10.1021/jp306037q | J. Phys. Chem. C XXXX, XXX, XXX−XXX

changed due to a lowering of the molecular symmetry, which induces a slight perturbation of the mean-field potential. For instance, on the basis of a mass spectroscopic study, Lievens and co-workers found that the $Pb_{12}Al^+$ cluster containing 50 valence electrons is a species with enhanced stability.[74] This special stability can be rationalized by considering the fact that a splitting of the $l = 4$ (F) shells in an icosahedral symmetry invariably lowers the energy level under crystal field effects.[75] This assumption was subsequently applied to rationalize the high stability of the doped group IVA clusters such as the clusters $X_{10}M^-$ (X = Ge, Sn, Pb and M = Cu, Ag, Au),[38,39] $Ge_{12}M^q$ (M = Li, Be, Mg, B, Al), and $Sn_{12}Zn$.[40]

The shape of the MOs and their energy levels of the Si_9B^- anion displayed in Figure 6a indicate that its 40 valence electrons are distributed in the following electron configuration:

$$[1(A_1')^2 1(A_2'')^2 1(E')^4 1(E'')^4 2(A_1')^4 2(E')^4 2(A_2'')^2 3(E')^4 2 (E'')^4 4(E')^4 3(A'')^2 3(A')^2 1(A_2')^2]$$

This corresponds to an energy sequence of electronic shell model as:

$$[1S^2 1P^6 1D^4 2S^2 1D^6 2P^6 1F^{14}]$$

The lowest MO is an s-type valence orbital, being followed by three p-type orbitals of the $1P^6$ subshell. Our analysis shows that the 1S-orbital is constructed by interaction between s-AO of B-atom and s-AOs of Si-atoms, while MOs of 1P subshells are mainly composed of s-AO(Si) and p-AOs of B-atom with much smaller contribution. The partial densities of states (pDOS) plots also reveal that the s-orbital of the 2S subshell is formed by a symmetric combination of 3s-AOs of Si and 2s-AO of B. This combination stabilizes the 2S subshell in pushing it deeper into the 1D subshell. More interestingly, the significant contributions of 2p-AOs of B and 3s-AOs of Si are also observed for the MOs of the 2P subshell. An analysis of canonical molecular orbital (CMO) indicates that while the MOs of the P-subshells contribute to both chemical bonds between B-impurity and Si_9 host and also to those of Si-atoms of the Si_9 host, the remaining MOs are only responsible for chemical bonding within the Si_9 host framework. Generally, although the 1D-subshell is split into the 2S-subshell due to the effect of B-impurity, the electronic configuration of the anion Si_9B^- basically satisfies the electron shell model of $[1S^2 1P^6 1D^{10} 2S^2 2P^6 1F^{14} 1G^0]$ and makes it an enhanced stability species with a magic number of 40 valence electrons.

A similar observation is also found for the cationic clusters $Si_{10}B^+$ (Figure 6b) containing 42 valence electrons with an electronic configuration of:

$$[(1A_1)^2 (1E)^4 (2A_1)^2 (3A_1)^2 (1B_1)^2 (2E)^4 (1B_2)^2 (4A_1)^2 (5A_1)^2 (3E)^4 (6A_1)^2 (4E)^4 (2B_1)^2 (4E)^4 (2B_2)^2 (7A_1)^2 (5E)^0]$$

This corresponds to the energy sequence of electronic shell model as:

$$[1S^2 1P^6 1D^{10} 2S^2 2P^6 1F^{14} 1G^2 1G^0]$$

Similar to the cases of the doped group IVA clusters previously reported, due to a symmetry lowering of the $Si_{10}B^+$ (C_{4v}) geometry, the G-subshell is now split and results in a large energy gap of 3.16 eV between the frontier orbitals, which ultimately leads to a large stabilization and high thermodynamic stability for the cation $Si_{10}B^+$.

The numbers of valence electrons of Si_4B^- and Si_8B^+ are 20 and 34, respectively, which are also magic numbers in JSM. However, our theoretical predictions point out that they are not emerged having an enhanced stability as the cases of Si_9B^- and $Si_{10}B^+$. Experimental studies that could be performed in the near future are expected to give more insights about the stability motif of these interesting systems.

Three-Dimensional Aromaticity. Aromaticity is well recognized as a measure of stability of chemical compounds. While aromaticity of planar structures can qualitatively be probed by using the classical Hückel rule of $(4n + 2)$ valence electrons,[76] the $2(N + 1)^2$ electron count rule, which is recently proposed by Hirsch et al.,[77] is proven to be an effective criterion for spherical structures. In the latter electron counting framework, the π-electron system of fullerenes can approximately be considered as a spherical electron gas, which surrounds the surface of a sphere (I_h). The wave functions of this electron gas can be characterized by the angular momentum quantum numbers ($l = 0, 1, 2, 3$, etc.) that are comparable to the atomic s, p, d, f orbitals. Accordingly, if a spherical system bearing $2(N + 1)^2$ π-electrons fully fills all π-shells, it then is stabilized and exhibits a certain aromatic character.

Let us consider the MO pictures of the global minimum of Si_9B^- depicted in Figure 6a. The valence orbitals of Si_9B^- can be divided into two subsets, the first containing the MOs of the shells [1S(A_1', σ), 1P(A_2'', σ), 1P(E', σ), 1D(E'', σ), 1D(A_1', σ), 1D(E', σ) and 1F(E'', σ), 1F(E', σ), 1F(A_2'', σ), 1F(A_1', σ) and 1F(A_2', σ)] that are occupied by 32 σ-electrons. The second subset includes the MOs of the shells [2S(A_1', π), 2P(A_2'', π), and 2P(E', π)], that are occupied by 8 valence π-electrons. As a consequence, this π-electron system make Si_9B^- a three-dimensional π-aromatic satisfying the $2(N + 1)^2$ electron count rule.

Similarly, the second subset of π-MOs of the cation $Si_{10}B^+$ also contains eight valence π-electrons (Figure 6b). Consequently, it satisfies the $2(N + 1)^2$ rule and then makes $Si_{10}B^+$ spherically aromatic. This aromatic feature can be regarded as one of the main reasons for the enhanced stability of Si_9B^- and $Si_{10}B^+$ as compared to the other sizes in the series of charged boron-doped silicon clusters.

CONCLUDING REMARKS

In this Article, we reported on a systematic investigation of the boron-doped silicon clusters Si_nB ($n = 1-10$) in the neutral, anionic, and cationic states using quantum chemical MO calculations. The global minima of the clusters considered are identified on the basis of the G4 energies. Total atomization energies, heats of formation, and the thermochemical derivatives such as ionization energy, electron affinity, dissociation energies, etc., are obtained using the high accuracy G4 and CCSD(T)/CBS methods. Some available experimental thermochemical values can be assessed. We thus determine for the first time a consistent and reliable set of values for the standard enthalpies of formation for the whole series of Si_nB.

The growth mechanism for boron-doped silicon clusters Si_nB with $n = 1-10$ can be established as follows:

(i) Each boron-doped silicon cluster Si_nB is formed by attaching the additional Si atom into the smaller size and doped $Si_{n-1}B$.

(ii) A competition between the exposed and the enclosed structures begins to occur at the size $n = 8$ (Si_8B).

dx.doi.org/10.1021/jp306037q | J. Phys. Chem. C XXXX, XXX, XXX−XXX

(iii) The larger size clusters such as Si_9B and $Si_{10}B$ exhibit the enclosed structures where the B-impurity is doped at the center of the corresponding Si_n host cage.

Our calculations also predict that the species Si_9B^-, Si_9B, and $Si_{10}B^+$ are characterized by an enhanced stability with high average binding energies and embedded energies. The higher stability of the closed shells Si_9B^- and $Si_{10}B^+$ can be rationalized in terms of the jellium shell model and their spherically aromatic character.

■ ASSOCIATED CONTENT

Supporting Information

Tables contain the single point electronic energies obtained at the CCSD(T)/auc-cc-pV*n*Z levels (n = Q, 5) and their CBS values. Cartesian coordinates of all low-lying isomers $Si_nB^{0/\pm}$ are obtained at the B3LYP (G4) level. Total G4 energies and TAEs of $Si_nB^{-/0/+}$. Total G4 energies of pure silicon clusters $Si_n^{0/\mp}$. This material is available free of charge via the Internet at http://pubs.acs.org.

■ AUTHOR INFORMATION

Corresponding Author

*E-mail: minh.nguyen@chem.kuleuven.be.

Notes

The authors declare no competing financial interest.

■ ACKNOWLEDGMENTS

M.T.N. is indebted to the KU Leuven Research Council (GOA, IDO, and IUAP programs) and thanks ICST at HoChiMinh City for supporting his stays in Vietnam. T.B.T. thanks the Arenberg Doctoral School for a scholarship.

■ REFERENCES

(1) (a) Zdetsis, A. D. *J. Chem. Phys.* **2007**, *127*, 014314/01−10. (b) Zdetsis, A. D. *J. Chem. Phys.* **2007**, *127*, 244308/01−06.
(2) Beck, S. M. *J. Chem. Phys.* **1987**, *87*, 4233−4234.
(3) Xu, H. G.; Wu, M. M.; Zhang, Z. G.; Yuan, J. Y.; Sun, Q.; Zheng, W. J. *J. Chem. Phys.* **2012**, *136*, 104308/01−10.
(4) Li, G. L.; Ma, W. L.; Gao, A. M.; Chen, H. Y.; Finlow, D.; Li, Q. S. *J. Theor. Comput. Chem.* **2012**, *11*, 185−196.
(5) Ziella, D. H.; Caputo, M. C.; Provasi, P. F. *Int. J. Quantum Chem.* **2011**, *111*, 1680−1693.
(6) Liu, T. G.; Zhao, G. F.; Wang, Y. X. *Phys. Lett. A* **2011**, *375*, 1120−1127.
(7) Ye, J. Z.; Li, B. X. *J. Phys. B* **2010**, *405*, 1461−1465.
(8) Xu, H. G.; Zhang, Z. G.; Feng, Y. A.; Zheng, W. J. *Chem. Phys. Lett.* **2010**, *498*, 22−26.
(9) Xu, H. G.; Zhang, Z. G.; Feng, Y.; Yuan, J. Y.; Zhao, Y. C.; Zheng, W. J. *Chem. Phys. Lett.* **2010**, *487*, 204−208.
(10) He, J. G.; Wu, K. C.; Sa, R. J.; Li, Q. H.; Wei, Y. Q. *Chem. Phys. Lett.* **2010**, *490*, 132−137.
(11) Fan, H. W.; Yang, J. C.; Lu, W.; Ning, H. M.; Zhang, Q. C. *J. Phys. Chem. A* **2010**, *114*, 1218−1223.
(12) (a) Zdetsis, A. D.; Koukaras, E. N.; Garoufalis, C. S. *J. Math. Chem.* **2009**, *46*, 971−980. (b) Zdetsis, A. D. *Inorg. Chem.* **2008**, *47*, 8823−8829. (c) Zdetsis, A. D. *J. Chem. Phys.* **2008**, *128*, 184305/01−07. (d) Zdetsis, A. D. *J. Phys. Chem. A* **2008**, *112*, 5712−5719. (e) Zdetsis, A. D. *Phys. Rev. B* **2007**, *75*, 085409/01−10.
(13) (a) Robles, R.; Khanna, S. N. *Phys. Rev. B* **2009**, *80*, 115414/01−05. (b) Robles, R.; Khanna, S. N. *J. Chem. Phys.* **2009**, *130*, 164313/01−06.
(14) Li, J. R.; Wang, G. H.; Yao, C. H.; Mu, Y. W.; Wan, J. G.; Han, M. *J. Chem. Phys.* **2009**, *130*, 164514/01−09.
(15) Li, B. X.; Wang, G. Y.; Ding, W. F.; Ren, X. J.; Ye, J. *Z. Phys. B: Condens. Matter* **2009**, *404*, 1679−1685.
(16) Lan, Y.-Z.; Feng, Y.-L. *Phys. Rev. A* **2009**, *79*, 033201/01−09.
(17) Hao, D. S.; Liu, J. R.; Wu, W. G.; Yang, J. C. *Theor. Chem. Acc.* **2009**, *124*, 431−437.
(18) Grubisic, A.; Ko, Y. J.; Wang, H.; Bowen, K. H. *J. Am. Chem. Soc.* **2009**, *131*, 10783−10790.
(19) Lin, L. H.; Yang, J. C.; Ning, H. M.; Hao, D. S.; Fan, H. W. *J. Mol. Struct. (THEOCHEM)* **2008**, *851*, 197−206.
(20) Li, X.; Wang, H.; Grubisic, A.; Wang, D.; Bowen, K. H.; Jackson, M.; Kiran, B. *J. Chem. Phys.* **2008**, *129*, 134309/01−04.
(21) Koyasu, K.; Atobe, J.; Furuse, S.; Nakajima, A. *J. Chem. Phys.* **2008**, *129*, 214301/01−07.
(22) Hossain, D.; Pittman, C. U.; Gwaltney, S. R. *Chem. Phys. Lett.* **2008**, *451*, 93−97.
(23) Hao, D.; Liu, J.; Yang, J. *J. Phys. Chem. A* **2008**, *112*, 10113−10119.
(24) Guo, L.-J.; Zhao, G.-F.; Gu, Y.-Z.; Liu, X.; Zeng, Z. *Phys. Rev. B* **2008**, *77*, 195417/01−08.
(25) Gruene, P.; Fielicke, A.; Meijer, G.; Janssens, E.; Vu, T. N.; Nguyen, M. T.; Lievens, P. *ChemPhysChem* **2008**, *9*, 703−706.
(26) Dkhissi, A. *Int. J. Quantum Chem.* **2008**, *108*, 996−1003.
(27) Cao, Y.; Hockendorf, R. F.; Beyer, M. K. *ChemPhysChem* **2008**, *9*, 1383−1386.
(28) Cao, T. T.; Feng, X. J.; Zhao, L. X.; Liang, X.; Lei, Y. M.; Luo, Y. H. *Eur. Phys. J. D* **2008**, *49*, 343−351.
(29) (a) Sporea, C.; Rabilloud, F. *J. Chem. Phys.* **2007**, *127*, 164306/01−07. (b) Sporea, C.; Rabilloud, F.; Cosson, X.; Allouche, A. R.; Aubert-Frecon, M. *J. Phys. Chem. A* **2006**, *110*, 6032−6038. (c) Sporea, C.; Rabilloud, F.; Allouche, A. R.; Frecon, M. *J. Phys. Chem. A* **2006**, *110*, 1046−1051.
(30) Koyasu, K.; Atobe, J.; Akutsu, M.; Mitsui, M.; Nakajima, A. *J. Phys. Chem. A* **2007**, *111*, 42−49.
(31) Janssens, E.; Gruene, P.; Meijer, G.; Woste, L.; Lievens, P.; Fielicke, A. *Phys. Rev. Lett.* **2007**, *99*, 063401/01−04.
(32) Dmytruk, A.; Park, Y. S.; Kasuya, A.; Kikuchi, H.; Takahashi, M.; Kawazoe, Y.; Watanabe, A. *J. Nanosci. Nanotechnol.* **2007**, *7*, 3788−3791.
(33) (a) Nigam, S.; Majumder, C.; Kulshreshtha, S. K. *J. Chem. Phys.* **2004**, *121*, 7756/01−08. (b) Nigam, S.; Majumder, C.; Kulshreshtha, S. K. *J. Chem. Phys.* **2006**, *125*, 074303/01−11.
(34) Ma, L.; Zhao, J.; Wang, J.; Wang, B.; Lu, Q.; Wang, G. *Phys. Rev. B* **2006**, *73*, 125439/01−08.
(35) Vu, T. N.; Gruene, P.; Claes, P.; Janssens, E.; Fielicke, A.; Nguyen, M. T.; Lievens, P. *J. Am. Chem. Soc.* **2010**, *132*, 15589−15602 and references therein..
(36) (a) Tam, N. M.; Ngan, V. T.; de Haeck, J.; Bhattacharyya, S.; Le, H. T.; Janssens, E.; Lievens, P.; Nguyen, M. T. *J. Chem. Phys.* **2012**, *136*, 024301/01−11. (b) De Haeck, J.; Bhattacharyya, S.; Le, H. T.; Debruyne, D.; Tam, N. M.; Ngan, V. T.; Janssens, E.; Nguyen, M. T.; Lievens, P. *Phys. Chem. Chem. Phys.* **2012**, *14*, 8542−8550.
(37) Vu, T. N.; Nguyen, M. T. *J. Phys. Chem. A* **2010**, *114*, 7609−7615.
(38) (a) Tai, T. B.; Nguyen, M. T. *J. Phys. Chem. A* **2011**, *115*, 9993−9999 and references therein. (b) Tai, T. B.; Nguyen, M. T. *Chem. Phys. Lett.* **2010**, *492*, 290−296.
(39) Tai, T. B.; Hue, M. T. N.; Nguyen, M. T. *Chem. Phys. Lett.* **2011**, *502*, 187−193.
(40) Tai, T. B.; Tam, N. M.; Nguyen, M. T. *Chem. Phys.* **2011**, *388*, 1−8.
(41) (a) Yamauchi, J.; Aoki, N.; Mizushima, I. *Phys. Rev. B* **1997**, *55*, R10245−R10252. (b) Yoshimoto, Y.; Suwa, Y. *Appl. Phys. Lett.* **2011**, *99*, 191901/01−03 and references therein.
(42) Ohmori, K.; Esashi, N.; Takao, M.; Sato, D.; Hayafuji, Y. *Appl. Phys. Lett.* **2005**, *87*, 112101/01−03.
(43) Viswanathan, R.; Schmude, R. W.; Gingerich, K. A. *J. Phys. Chem.* **1996**, *100*, 10784−10786.
(44) Davy, R.; Skoumbourdis, E.; Dinsmore, D. *Mol. Phys.* **2005**, *103*, 611−619.
(45) Sun, Z.; Yang, Z.; Gao, Z.; Tang, Z. C. *Rapid Commun. Mass Spectrom.* **2007**, *21*, 792−798.

(46) Tai, T. B.; Kadlubanski, P.; Roszak, S.; Majumdar, D.; Leszczynski, J.; Nguyen, M. T. *ChemPhysChem* **2011**, *12*, 2948−2958.
(47) Frisch, M. J.; Schlegel, H. B.; Scuseria, G. E.; Robb, M. A.; Cheeseman, J. R.; Montgomery, J. A., Jr.; Vreven, T.; Kudin, K. N.; Burant, J. C.; Millam, J. M.; et al. *Gaussian 09*, revision B.01; Gaussian, Inc.: Wallingford, CT, 2009.
(48) Werner, H.-J.; Knowles, P. J.; Lindh, R.; Manby, F. R.; Schütz, M.; Celani, P.; Korona, T.; Rauhut, G.; Amos, R. D.; et al. *MOLPRO, version 2006.1, a package of ab initio programs*, 2006.
(49) Becke, A. D. *J. Chem. Phys.* **1993**, *98*, 5648−5652.
(50) Perdew, J. P.; Chevary, J. A.; Vosko, S. H.; Jackson, K. A.; Pederson, M. R.; Singh, D. J.; Fiolhais, C. *Phys. Rev. B* **1992**, *46*, 6671−6687.
(51) Clark, T.; Chandrasekhar, J.; Spitznagel, G. W.; Schleyer, P. V. *J. Comput. Chem.* **1983**, *4*, 294−301.
(52) Mclean, A. D.; Chandler, G. S. *J. Chem. Phys.* **1980**, *72*, 5639−5648.
(53) Frisch, M. J.; Pople, J. A.; Binkley, J. S. *J. Chem. Phys.* **1984**, *80*, 3265−3269.
(54) Peterson, K. A.; Xantheas, S. S.; Dixon, D. A.; Dunning, T. H. *J. Phys. Chem. A* **1998**, *102*, 2449−2454.
(55) (a) Tai, T. B.; Grant, D. J.; Nguyen, M. T.; Dixon, D. A. *J. Phys. Chem. A* **2010**, *114*, 994. (b) Nguyen, M. T.; Matus, M. H.; Ngan, V. T.; Grant, D. J.; Dixon, D. A. *J. Phys. Chem. A* **2009**, *113*, 4895. (c) Tai, T. B.; Tam, N. M.; Nguyen, M. T. *Theor. Chem. Acc.* **2012**, *131*, 1241/01−15.
(56) Curtiss, L. A.; Redfern, P. C.; Raghavachari, K. *J. Chem. Phys.* **2007**, *126*, 084108/01−12.
(57) Bartlett, R. J.; Musial, M. *Rev. Mod. Phys.* **2007**, *79*, 291−352.
(58) (a) Dunning, T. H. *J. Chem. Phys.* **1989**, *90*, 1007−1023. (b) Kendall, R. A.; Dunning, T. H.; Harrison, R. J. *J. Chem. Phys.* **1992**, *96*, 6796−6806. (c) Woon, D. E.; Dunning, T. H. *J. Chem. Phys.* **1993**, *98*, 1358−1371.
(59) Rittby, M.; Bartlett, R. J. *J. Phys. Chem.* **1988**, *92*, 3033−3036.
(60) Deegan, M. J. O.; Knowles, P. J. *Chem. Phys. Lett.* **1994**, *227*, 321−326.
(61) (a) Peterson, K. A.; Dunning, T. H., Jr. *J. Chem. Phys.* **2002**, *117*, 10548. (b) Woon, D. E.; Dunning, T. H., Jr. *J. Chem. Phys.* **1993**, *98*, 1358.
(62) (a) Helgaker, T.; Klopper, W.; Koch, H.; Noga, J. *J. Chem. Phys.* **1997**, *106*, 9639−9646. (b) Halkier, A.; Helgaker, T.; Jorgensen, P.; Klopper, W.; Koch, H.; Olsen, J.; Wilson, A. K. *Chem. Phys. Lett.* **1998**, *286*, 243−252.
(63) (a) Douglas, M.; Kroll, N. M. *Ann. Phys.* **1974**, *82*, 89−155. (b) Hess, B. A. *Phys. Rev. A* **1985**, *32*, 756−763. (c) Hess, B. A. *Phys. Rev. A* **1986**, *33*, 3742−3748.
(64) de Jong, W. A.; Harrison, R. J.; Dixon, D. A. *J. Chem. Phys.* **2001**, *114*, 48−53.
(65) EMSL basis set library: http://www.emsl.pnl.gov/forms/basisform.html.
(66) Moore, C. E. *Atomic Energy Levels As Derived from the Analysis of Optical Spectra*; U.S. National Bureau of Standards Circular 467, U.S. Department of Commerce, National Technical Information Service, COM-72-50282: Washington, DC, 1949; Vol. *1H to V*.
(67) Karton, A.; Martin, J. M. L. *J. Phys. Chem. A* **2007**, *111*, 5936−5944.
(68) Curtiss, L. A.; Raghavachari, K.; Redfern, P. C.; Pople, J. A. *J. Chem. Phys.* **1997**, *106*, 1063−1079.
(69) Boldyrev, A. I.; Simons, J. *J. Phys. Chem.* **1993**, *97*, 1526−1532.
(70) (a) Kumar, V.; Kawazoe, Y. *Appl. Phys. Lett.* **2003**, *83*, 2677−2679. (b) Kumar, V.; Kawazoe, Y. *Phys. Rev. Lett.* **2001**, *87*, 045503/01−04. (c) Kumar, V.; Singh, A. K.; Kawazoe, Y. *Phys. Rev. B* **2006**, *74*, 125411/01−05. (d) Kumar, V.; Kawazoe, Y. *Phys. Rev. B* **2002**, *65*, 073404/01−04.
(71) Bai, J.; Cui, L. F.; Wang, J. L.; Yoo, S. H.; Li, X.; Jellinek, J.; Koehler, C.; Frauenheim, T.; Wang, L. S.; Zeng, X. C. *J. Phys. Chem. A* **2006**, *110*, 908−912.
(72) Brack, M. *Rev. Mod. Phys.* **1993**, *65*, 677−732.
(73) (a) Tai, T. B.; Nguyen, M. T. *J. Comput. Chem.* **2012**, *33*, 800−809. (b) Tai, T. B.; Nguyen, M. T. *J. Chem. Theory Comput.* **2011**, *7*, 1119−1130. (c) Tai, T. B.; Nguyen, M. T. *Chem. Phys. Lett.* **2010**, *489*, 75−80. (d) Tai, T. B.; Nhat, P. V.; Nguyen, M. T.; Li, S. G.; Dixon, D. A. *J. Phys. Chem. A* **2011**, *115*, 7673−7686. (e) Tai, T. B; Nhat, P. V.; Nguyen, M. T. *Phys. Chem. Chem. Phys.* **2010**, *12*, 11477−11486.
(74) Neukermans, S.; Janssens, E.; Chen, Z. F.; Silverans, R. E.; Schleyer, P. v. R.; Lievens, P. *Phys. Rev. Lett.* **2004**, *92*, 163401/01−04.
(75) Schriver, K. E.; Persson, J. L.; Honea, E. C.; Whetten, R. L. *Phys. Rev. Lett.* **1990**, *64*, 2539−2542.
(76) Boldyrev, A. I.; Wang, L. S. *Chem. Rev.* **2005**, *105*, 3716−3757.
(77) Hirsch, A.; Chen, Z.; Jiao, H. *Angew. Chem., Int. Ed.* **2000**, *39*, 3915−3917.